This document was prepared in conjunction with work accomplished under Contract No. DE-AC09-96SR18500 with the U. S. Department of Energy.

Plutonium Oxidation and Subsequent Reduction by Mn(IV) Minerals

Brian A. Powell[1*], Martine C. Duff[2], Paul. M. Bertsch[3], John T. Coates[1], Peter. Eng[4], Robert A. Fjeld[1], Douglas B. Hunter[2], Daniel I. Kaplan[2], Matthew Newville[4], Mark. L. Rivers[4], Steven M. Serkiz[2], Stephen R. Sutton[4], Ines R. Triay[5], and David T. Vaniman[6]

1. Department of Environmental Engineering and Science, Clemson University, Anderson, SC 29630
2. Savannah River National Laboratory, Aiken, SC 29808
3. Savannah River Ecology Laboratory, The University of Georgia, Aiken, SC 29808
4. Department of Geophysical Sciences and Center for Advanced Radiation Sources, The University of Chicago, Chicago, IL 60637
5. Waste Isolation Pilot Plant, Carlsbad, NM 88221
6. Los Alamos National Laboratory, Los Alamos, NM 87545

*To whom correspondence should be addressed: Current Address: BAPowell@lbl.gov (510) 486-5377 Lawrence Berkeley National Laboratory, Berkeley, CA 94730

Keywords. Plutonium, Pu, manganese oxide, pyrolusite, solvent extraction, tuff, XANES, Yucca Mountain Site, radioactive waste management

Synopsis. Aqueous plutonium(V) initially oxidizes and then eventually undergoes reduction when it comes in contact with Mn(IV) minerals.

Abstract. Plutonium sorbed to rock tuff was preferentially associated with manganese oxides. On tuff and synthetic pyrolusite ($Mn^{IV}O_2$), Pu(IV) or Pu(V) was initially oxidized, but over time Pu(IV) became the predominant oxidation state of sorbed Pu. Reduction of Pu(V/VI), even on non-oxidizing surfaces, is proposed to result from a lower Gibbs free energy of the hydrolyzed Pu(IV) surface species versus that of the Pu(V) or Pu(VI) surface species. This work suggests that despite initial oxidation of sorbed Pu by oxidizing surfaces to more soluble forms, the less mobile form of Pu, Pu(IV), will dominate Pu solid phase speciation during long term geologic storage.

The safe design of a radioactive waste or spent nuclear fuel geologic repository requires a risk assessment of radionuclides that may potentially be released into the surrounding environment. Geochemical knowledge of the radionuclide and the surrounding environment is required for predicting subsurface fate and transport. Although difficult even in simple systems, this task grows increasingly complicated for constituents, like Pu, that exhibit complex environmental chemistries. The environmental behavior of Pu can be influenced by complexation, precipitation, adsorption, colloid formation, and oxidation/reduction (redox) reactions (*1-3*). To predict the environmental mobility of Pu, the most important of these factors is Pu oxidation state. This is because Pu(IV) is generally 2 to 3 orders of magnitude less mobile than Pu(V) in most environments (*4*). Further complicating matters, Pu commonly exists simultaneously in several oxidation states (*5, 6)*. Choppin (*7*) reported Pu may exist as Pu(IV), Pu(V), or Pu(VI) oxic natural groundwaters. It is generally accepted that plutonium associated with suspended particulate matter is predominantly Pu(IV) (*8-10*), whereas Pu in the aqueous phase is predominantly Pu(V) (*2, 11-13*).

The influence of the character of Mn-containing minerals expected to be found in subsurface repository environments on Pu oxidation state distributions has been the subject of much recent research. Kenney-Kennicutt and Morse (*14*), Duff *et al*. (*15*), and Morgenstern and Choppin (*16*) observed oxidation of Pu facilitated by Mn(IV)-bearing minerals. Conversely, Shaughnessy *et al*. (*17*) used X-ray Absorption near-edge spectroscopy (XANES) to show reduction of Pu(VI) by hausmannite ($Mn^{II}Mn^{III}_2O_4$) and manganite (γ-$Mn^{III}OOH$) and Kersting *et al*., (*18*) observed reduction of Pu(VI) by pyrolusite ($Mn^{IV}O_2$). In this paper, we attempt to reconcile the apparently conflicting datasets by showing that Mn-bearing minerals can indeed oxidize Pu, however, if the oxidized species remains on the solid phase, the oxidation step competes with the formation of Pu(IV) that becomes the predominant solid phase Pu species with time. The experimental approach we took was to conduct longer term (approximately two years later) oxidation state analyses on the Pu sorbed to Yucca Mountain tuff (initial analysis reported by Duff *et al*., (*15*)) and measure the time-dependant changes in the oxidation state distribution of Pu in the presence of the Mn mineral pyrolusite.

Yucca Mountain Tuff Experiments. Duff *et al.* (*15*) observed oxidation of Pu(V) to Pu(VI) following sorption to a natural zeolitic tuff using micro-XANES. The tuff contained trace quantities of iron and manganese oxides. Using synchrotron based micro-X-ray fluorescence (micro-SXRF), it was shown that Pu was preferentially associated with Mn oxides (specifically, ranciete, $(Ca^{+2},Mn^{+2})OMn^{IV}O_2 \cdot 3H_2O$) and smectites rather than with iron oxides or zeolites. These measurements were performed two and six months after adding aqueous Pu(V) to the tuff. In the present work, the tuff was again analyzed by XANES. At the time of analysis, two years had passed since the aqueous Pu(V) was added to the tuff. As shown in Figure 1, the predominant solid phase species after two years was Pu(IV). Additionally, the Pu was still associated with the mineral phases containing Mn(IV) at an estimated loading of 2000 mg Pu kg^{-1} at the Mn-rich regions on the tuff. Therefore, the Pu, initially added as Pu(V), was oxidized to Pu(VI) then reduced to Pu(IV). Additionally, EXAFS spectra indicated that sorbed Pu was coordinated with the Mn surface rather than precipitated as a Pu (hydr)oxide (*19*). Therefore, the mechanism of reduction was not associated with the formation of a discrete Pu-hydroxide solid. Rather the reduction appears to be facilitated by the solid phase. These data from aged samples appear to conflict with observations that Mn(IV)-containing minerals are capable of oxidizing Pu (*15*, *16*). To further examine this phenomenon, batch sorption experiments were designed to study the interactions between Pu and a synthetic Mn(IV) mineral as a function of time and bulk solution pH. The pyrolusite was prepared by the method of McKenzie (*20*) and the characterization data for this solid are presented in the Online Supporting Material.

Pyrolusite Experiments. A plot of sorbed Pu versus time and pH in pyrolusite suspensions is presented in Figure 2. At all pH values, a large fraction of the Pu was sorbed within 5 min, ranging from 0.6 at pH 2.6 to >0.8 at pH 8.2. This was followed by a period in which the sorbed Pu decreased for pH values of 2.6 and 3.4 and increased for pH 4.8 and 8.2. After seven days almost all of the Pu in pH 4.8 and 8.2 systems was sorbed.

Insight into the processes responsible for these observations can be gleamed from the analysis of the Pu oxidation state in the pH 2.6 and 8.2 systems (Figure 3). Pu oxidation state analysis was performed as a function of time on the aqueous phase and the total system (defined as the oxidation state in both the solid and aqueous phase combined) using ultra-filtration and solvent extraction techniques. Details of the experimental technique are provided in the Online Supporting Material and are reported elsewhere (*21*, *22*). Oxidation of Pu(IV) at pH 2.6 occurs with a steady decline of Pu(IV) and corresponding increases in Pu(V) and Pu(VI) (Figure 3a). During these experiments, no Pu(IV) was measured in the aqueous phase of suspensions–suggesting that Pu(IV) was oxidized on the pyrolusite surface and subsequently partitioned into the aqueous phase as Pu(V/VI). The oxidation followed by desorption process was deduced from the decrease in the fraction of Pu sorbed (Figure 2) and the increase in the fraction of Pu(V/VI) in the system (Figure 3a).

Soon after adding Pu(IV) in the pH 8.2 system (Figure 3b), there was a slight increase in the fraction of Pu(V) and Pu(VI). During the first 60 min when Pu(V) and Pu(VI) were present, a small fraction of Pu desorbed into the aqueous phase. Similar to the experiment at pH 2.6, no Pu(IV) was measured in the aqueous phase, indicating a surface mediated reaction (discussed below). With time, however, the oxidized Pu re-sorbed to the pyrolusite surface and was reduced to Pu(IV). Although these data demonstrate that pyrolusite oxidizes Pu(IV) to Pu(V/VI), with Pu(V/VI) remaining sorbed to the mineral surface ultimately being reduced to Pu(IV). These data lead us to conclude that Pu in the aqueous phase of a pyrolusite suspension will be Pu(V) or Pu(VI). Likewise, Pu sorbed to the solid phase will be reduced to or remain sorbed as Pu(IV). These results are consistent with the XANES analysis of the oxidation state distribution of sorbed Pu to natural Mn(IV) phases within YM tuff (Figure 1).

To further examine the effect of pH in these systems, pH sorption edge experiments were conducted to provide information about the Pu oxidation state distribution after 30 days of equilibration in pyrolusite suspensions amended with Pu(IV) and Pu(V). The total system Pu oxidation state distribution after 30 days in pyrolusite systems is shown in Figure 4. The data sets are nearly identical, irrespective of the initial Pu oxidation state (added as either Pu(IV) or Pu(V)). Comparing the distribution of Pu(V) and Pu(VI) in the total system with the sorbed Pu (Figure 4 insert) there is a correlation between the fraction of oxidized Pu in the system and the Pu concentration in the aqueous phase (unshaded area in Figure 4 insert). In fact, all of the Pu in the aqueous phase was either Pu(V) or Pu(VI) (data not shown). At low pH values, Pu(IV) and Pu(V) appear to be oxidized on the mineral surface and partition between the aqueous and solid phase as Pu(V) and Pu(VI). The solid phase oxidation state distribution indicated that Pu(IV) was the predominant solid phase oxidation state following addition of either Pu(IV) or Pu(V). Above a pH of 3, all Pu species partitioned to the pyrolusite surface and reduced to Pu(IV), or remained sorbed as Pu(IV) when Pu was added as Pu(IV).

It was difficult to explain the formation of reduced Pu(IV) on Mn(IV) oxides, so a similar kinetic study was repeated using glass beads, with presumably little or no redox active surface (presented in On-Line Supporting Material). The glass beads were first washed in a basic solution then in an acidic bath to decrease the likelihood of an organic or inorganic contaminant. There was a decrease in the fraction of Pu(V) in the system with a corresponding increase in the fraction of Pu(IV), indicating that Pu(V) was being reduced. The changes in Pu oxidation state were very similar to those observed for pyrolusite, except the reaction kinetics were much slower. Analysis of Pu in the aqueous phase showed no Pu(IV), indicating that reduction in the system did not occur until Pu was sorbed to the glass beads. The reduction of Pu(V) by glass observed in these experiments is similar to the observation by Kersting *et al.* (*12*) of Pu(V) reduction by SiO_2 using XANES. These are independent observations using different techniques, both of which show the development of sorbed Pu(IV) surface species.

The redox capacity of the pyrolusite used in these experiments was measured by iodometric titration using the method of Carpenter (*23*) and Murray *et al.*, (*24*). The redox capacity, which can be related to the average Mn oxidation state, was $2.41 \pm 0.11 \times 10^{-2}$ equivalents g^{-1}. This corresponds to a Mn:O ratio of 1.95 ± 0.03, instead of the ideal ratio of 2.00. Therefore, some Mn(II) or Mn(III) may have been present in the pyrolusite, providing an electron source for Pu(V/VI) reduction.

Proposed Pu Reduction Mechanism. Oxidation of Pu appears to be favored as long as it is desorbed from the mineral surface or weakly electrostatically adsorbed. It appears that oxidation of Pu by Mn oxide solids competes with reduction of Pu to a thermodynamically stable Pu(IV) solid phase species. This proposed mechanism is supported by the observations that 1) regardless of the initial aqueous Pu oxidation state added to a system, similar oxidation state distributions were obtained after 30 days of contact in pyrolusite suspensions, 2) initial oxidation followed by reduction was observed in pyrolusite and tuff systems, 3) reduction of Pu(V) was observed in pyrolusite suspensions despite the observed oxidizing capacity of Mn(IV) oxides, and 4) Pu(V) or Pu(VI) remaining on the solid phase of both tuff and synthetic pyrolusite eventually reduces to Pu(IV).

The stability of Pu(IV), even on an oxidizing surface, is proposed to be due to the formation of stable Pu(IV) hydrolyzed species. Although the observation of Pu(IV) on pyrolusite is surprising, it has been reported previously by Kersting *et al.* (*18*). An explanation may lie in a discussion from Morgenstern and Choppin (*16*), who were studying oxidation of Pu(IV) by a synthetic manganese dioxide ($Mn^{IV}O_2$, crystalline structure unknown). They observed that Pu(IV) was oxidized to Pu(V) and Pu(VI) at low pH (2.0 to 3.5), but oxidation was inhibited at high pH (8.0) values. Inhibition of oxidation at higher pH was attributed to the stabilization of Pu(IV) as the fully hydrolyzed species $Pu(OH)_4(aq)$. Significant amounts of $Pu(OH)_4(aq)$ have been shown to be present at pH values as low as 4 (*25*). Since hydrolysis will change the redox potential of a given Pu species, Pu reduction on a mineral surface is dependent on both Pu speciation/hydrolysis at the mineral surface as well as the redox capacity of the surface. It is possible that hydrolyzed Pu(IV) may be more energetically favorable on a mineral surface than Pu(V) because the favorable Gibbs free energy of the hydrolyzed Pu(IV) surface species (corresponding Gibbs free energy from homogenous solution: $\Delta Gf^{o}_{298} = -1377.5$ kJ mol^{-1} for $Pu(OH)_4(aq)$ compared with $\Delta Gf^{o}_{298} = -1039.1$ kJ mol^{-1} for $PuO_2OH(aq)$ (*13*)). Therefore, Pu(IV) hydrolysis, and possibly precipitation, may be the driving force for the observed stability of Pu(IV) on the mineral surface, through the formation of a stable inner sphere surface complex of Pu(IV) with surface hydroxyl groups. This is supported by the observation of Pu(V) reduction on glass beads as well as the stability of Pu(IV) on an oxidizing surface such as pyrolusite.

This mechanism by which the hydrolysis of Pu at the mineral surface lowers the Gibbs free energy sufficiently to make the reduction of Pu(V) thermodynamically favorable is similar to that put forth by Wan *et al.* (*26*), where they observed the reoxidation of bioreduced uranium under reducing conditions. Microbial respiration produced (bi)carbonate and re-oxidation of uranium occurred due to the thermodynamic favorability of U(VI) carbonate complexes, although microbially mediated U(VI) reduction to U(IV) was initially observed and the community was sustained throughout the experiment.

The oxidation and reduction of Pu observed in these systems are competing reactions that likely occur through different reaction pathways. The effective charge for Pu species decreases in the order $Pu(IV)^{+4}$, $Pu(VI)O_2^{+2}$, $Pu(V)_2^{+}$; making Pu(IV) more attracted to a negatively charged surface than Pu(V). Additionally, while Pu(V) and Pu(VI) likely adsorb as outer-sphere complexes (consistent with the ability to quantitatively leach penta- and hexavalent actinides into solution by lowering the aqueous phase pH to 1.5, as done in this work), Pu(IV) adsorption is generally described as a irreversible process with formation of an inner-sphere complex. These two adsorption mechanisms likely have a significant impact on Pu oxidation state transformations. It is possible that formation of an inner-sphere Pu surface complex involves reduction of Pu(V/VI) to Pu(IV) where reduction may be facilitated by trace Mn(II) (or other reducing sites) within the mineral either by shuttling an electron through the crystal lattice or by adsorption and subsequent electron transfer from a specific Mn(II) site. Additionally, the eventual loss of water from the hydration sphere upon formation of a Pu(IV) surface complex may provide a barrier against eventual Pu(IV) re-oxidation. . The mechanisms proposed are largely speculative, based on long-term experimental observations and theoretical thermodynamic considerations. To truly describe the interfacial reactions occurring in these systems, techniques capable of investigating the mineral-water interface in real-time are required.

Summary. The knowledge that Mn(IV) minerals oxidize Pu into the more mobile form has required regulators and risk assessors to assume that disposed Pu at some radiological waste repositories will be more mobile than may in fact be the case. This study showed that, at neutral pH levels, Pu(V) oxidation by Mn(IV)-containing minerals occurs for only very short duration, and then even under oxidizing conditions, conditions that may exists in a vadose zone, the Pu becomes reduced to the less mobile form. From the point of view of risk estimates of buried waste (performance assessments), the durations that the Pu becomes oxidized by Mn(IV), in the order of days to <2 years, are extremely short compared to times of compliance of tens-of-thousands of years. This study has not only shown that Pu will sorb more strongly and therefore be less mobile in these repository settings containing Mn(IV) minerals, it lends itself to a new conceptual geochemical model that can be easily parameterized for performance assessments to more accurately predict the risk associated with the disposal of Pu-containing waste.

References.

1. G. R. Choppin and B. E. Stout, *Sci. Total Environ.* **83**, 377-396 (1989).
2. J. W. Morse and G. R. Choppin, *Rev. Aquat. Sci.* **4**, 1-22 (1991).
3. R. J. Silva and H. Nitsche, *Radiochim. Acta* **70-71**, 377-396 (1995).

4. Based upon distribution coefficients measured reported by D. M. Nelson, M. B. Lovett, *Nature* 276, 599-601, (1978).
5. J. M. Cleveland, *The Chemistry of Plutonium* (American Nuclear Society, La Grange Park, IL, 1979), pp. 291-322.
6. F. Weigel, J. J. Katz, G. T. Seaborg, in *The Chemistry of the Actinide Elements*, J. J. Katz, G. T. Seaborg, L. R. Morss, Eds. (Chapman & Hall, New York, NY 1986), vol. 1, pp. 680-702.
7. G. R. Choppin, *Radiochim. Acta* **91**, 645-649 (2003).
8. W. R. Penrose, D. N. Metta, J. M. Hylko, L. A. Rinckel, *J. Environ. Radio.* **5**, 169–184 (1987).
9. P. E. Mitchell, J. V. Battle, A. B. Downes, O. M. Bondren, L. L. Vintro, J. A. Sanchez-Cabeza, *Appl. Rad. Isot.* **46**, 1175-1190 (1995).
10. P. J. Kershaw, D. S. Woodhead, M. B. Lovett, K. S. Leonard, Appl. Rad. Isot. 46, 1121-1134 (1995).
11. K. A. Orlandini, W. R. Penrose, D. M. Nelson, *Mar. Chem.* **18**, 49-57 (1986).
12. D. McCubbin and K. S. Leonard, *J. Radioanal. Nucl. Chem.* **172**, 363-370 (1993).
13. W. Runde, S. D. Conradson, D. W. Efurd, N. Lu, C. E. VanPelt, C. D. Tait, *App. Geochem.* **17**, 837-853 (2002).
14. W. L. Kenney-Kennicutt and J. W. Morse, *Geochim. Cosmochim. Acta* **49**, 2577-2588 (1985).
15. M. C. Duff, D. B. Hunter, I. R. Triay, P. M. Bertsch, D. T. Reed, S. R. Sutton, G. Shea-McCarthy, J. Kitten, P. Eng, S. J. Chipera, D. T. Vaniman, *Environ. Sci. Tech.* **33**, 2163-2169 (1999).
16. A. Morgenstren and G. R. Choppin, *Radiochim. Acta* **90**, 69-74 (2002).
17. D. A. Shaughnessy, H. Nitsche, C. H. Booth, D. K. Shuh, G. A. Waychunas, R. E. Wilson, H. Gill, K. J. Cantrell, R. J. Serne, *Environ. Sci. Technol.* **37**, 3367-3374 (2003).
18. A. B. Kersting, P. Zhao, M. Zavarin, E. R. Sylwester, P. G. Allen, R. W. Williams, In *Rep. UCRL-ID-149688, Colloidal-Facilitate Transport of Low-Solubility Radionuclides: A Field, Experimental, and Modeling Investigation;* A. B. Kersting, P. W. Remus Eds. (Lawrence Livermore National Laboratory, Livermore, CA, 2003) pp. 67-87.
19. M. C. Duff, M. Newville, D. B. Hunter, S. R. Sutton, I. R. Triay, D. T. Vaniman, P. M. Bertsch, P. Eng, M. L. Rivers, In *APS Forefront;* G. K. Shenoy Ed. (Argonne National Laboratory, Argonne, IL 2001) pp. 18-21.
20. P. E. Mckenzie, *Mineral. Mag.* **38**, 493-502 (1971).
21. B. A. Powell, R. A. Fjeld, D. I. Kaplan, J. T. Coates, S. M. Serkiz, *Environ. Sci Tech.* **38**, 6016-6024 (2004).
22. B. A. Powell, R. A. Fjeld, D. I. Kaplan, J. T. Coates, S. M. Serkiz, *Environ. Sci Tech.* **39**, 2107-2114 (2005).
23. J. H. Carpenter, *Lumin. Ocean.* **10**, 141-143 (1965).
24. J. W. Murray, L.S. Balistrieri, B. Paul, *Mineral. Magazine* **38**, 493-502 (1971).
25. G. R. Choppin, A. H. Bond, P. M. Hromadka, *J. of Radio. Nucl. Chem.* **219** 203-210 (1997).
26. J. Wan, T. K. Tokunaga, E Brodie, Z Wang., Z. Zheng, D. Herman, T. C. Hazen, M K. Firestone, S. R. Sutton, *Environ. Sci. Tech.* **39**, 6162-6169 (2005).

27. This research was supported in part by the South Carolina Universities Research and Education Foundation (SCUREF) under the U.S. Department of Energy contract DE-FC09-00SR22184- Cooperative Agreement DOES0015, “Radiochemistry Education Award Program (REAP II)”. Additionally, this work was supported in part by DOE’s Environmental Management Science Program (EMSP), DOE’s Independent R&D Program, and SRNL’s mini-sabbatical program. The authors thank the Clemson University Chemistry Department for the use of their XRD spectrometer and Dr. Seyed Dashgheib of Clemson University for his assistance in collecting the surface area measurement of the manganese minerals used in this study. Portions of this work were performed at GeoSoilEnviro-CARS (GSE-CARS), Sector 13, Advanced Photon Source (APS). GSECARS is supported by the National Science Foundation-Earth Sciences, U.S. Dept. of Energy-Geosciences, W.M. Keck Foundation, and the U.S. Dept. of Agriculture. Use of the APS was supported by the U.S. Dept. of Energy, Basic Energy Sciences, Office of Energy Research, under Contract No. W-31-109-Eng-38. The research was also supported by Financial Assistance Award No. DE-FC09-96SR18546 from the U.S. Dept. of Energy to the University of Georgia Research Foundation.

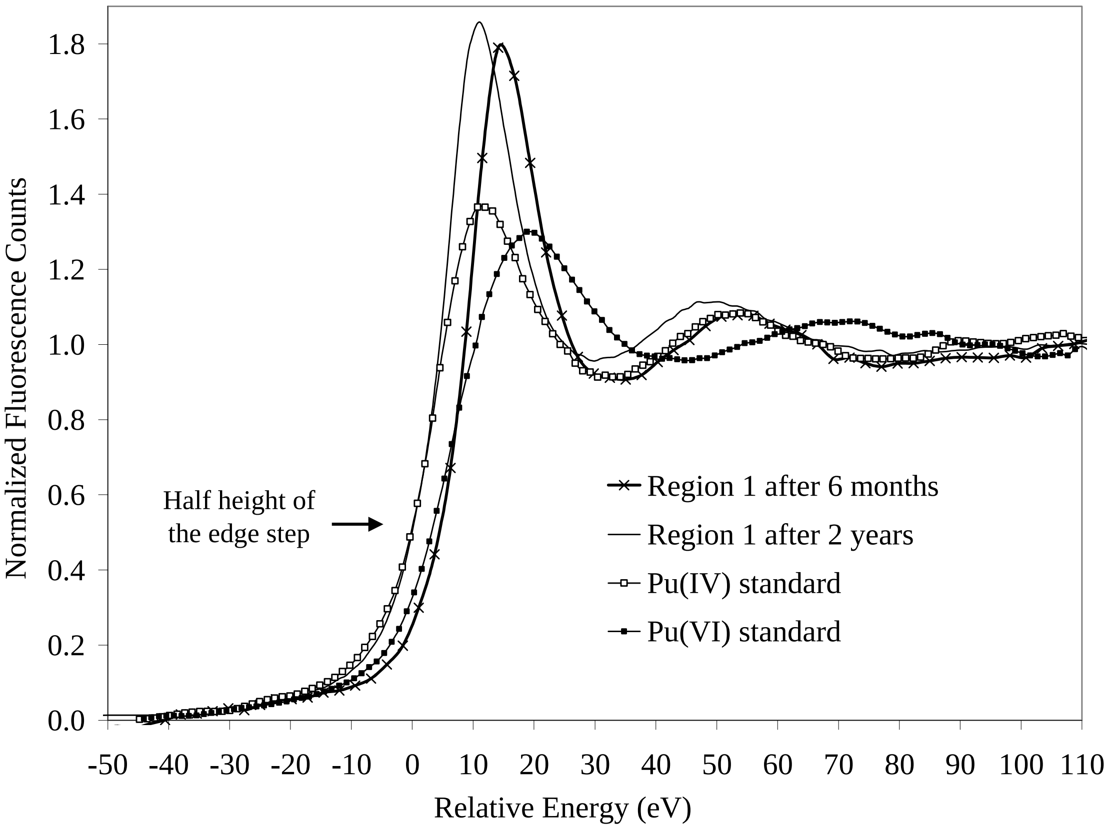

FIGURE 1: Plutonium L_3-edge XANES spectra plotted with respect to the relative XANES edge energy for sorbed Pu on YM tuff at six months and two years. All spectra taken after two years indicated an average oxidation state of Pu(IV); those taken after six months had average oxidation states predominantly of Pu(V) and Pu(VI)

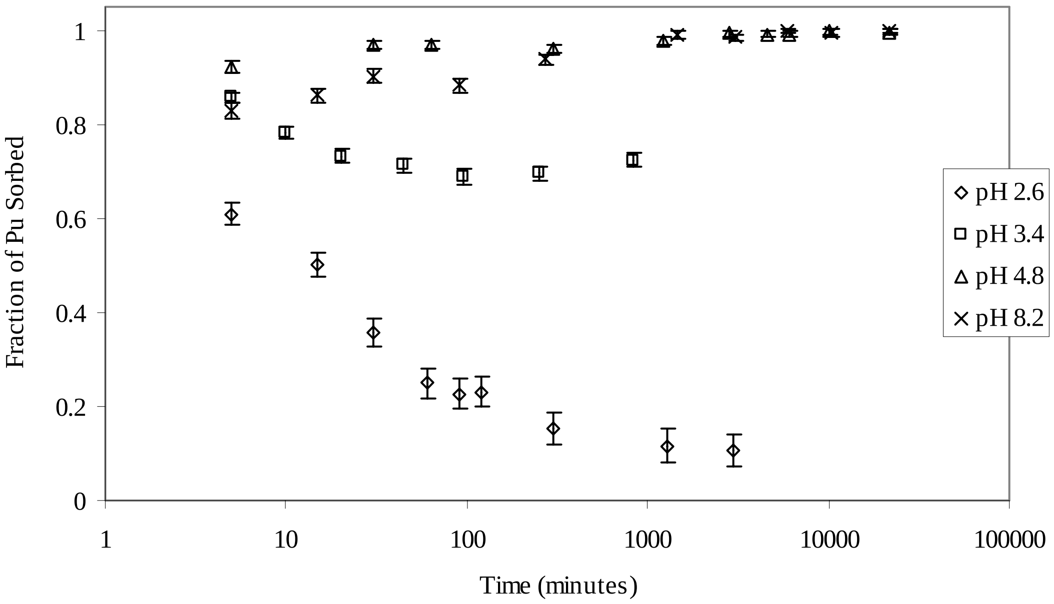

FIGURE 2: Fraction of sorbed Pu versus time in 10 $m^2 L^{-1}$ (4.00 ± 0.04 g L^{-1}) pyrolusite solutions at varying pH levels ([NaCl] = 0.01 M; initially added Pu(IV) at [Pu] = 6.1 x 10^{-11} M).

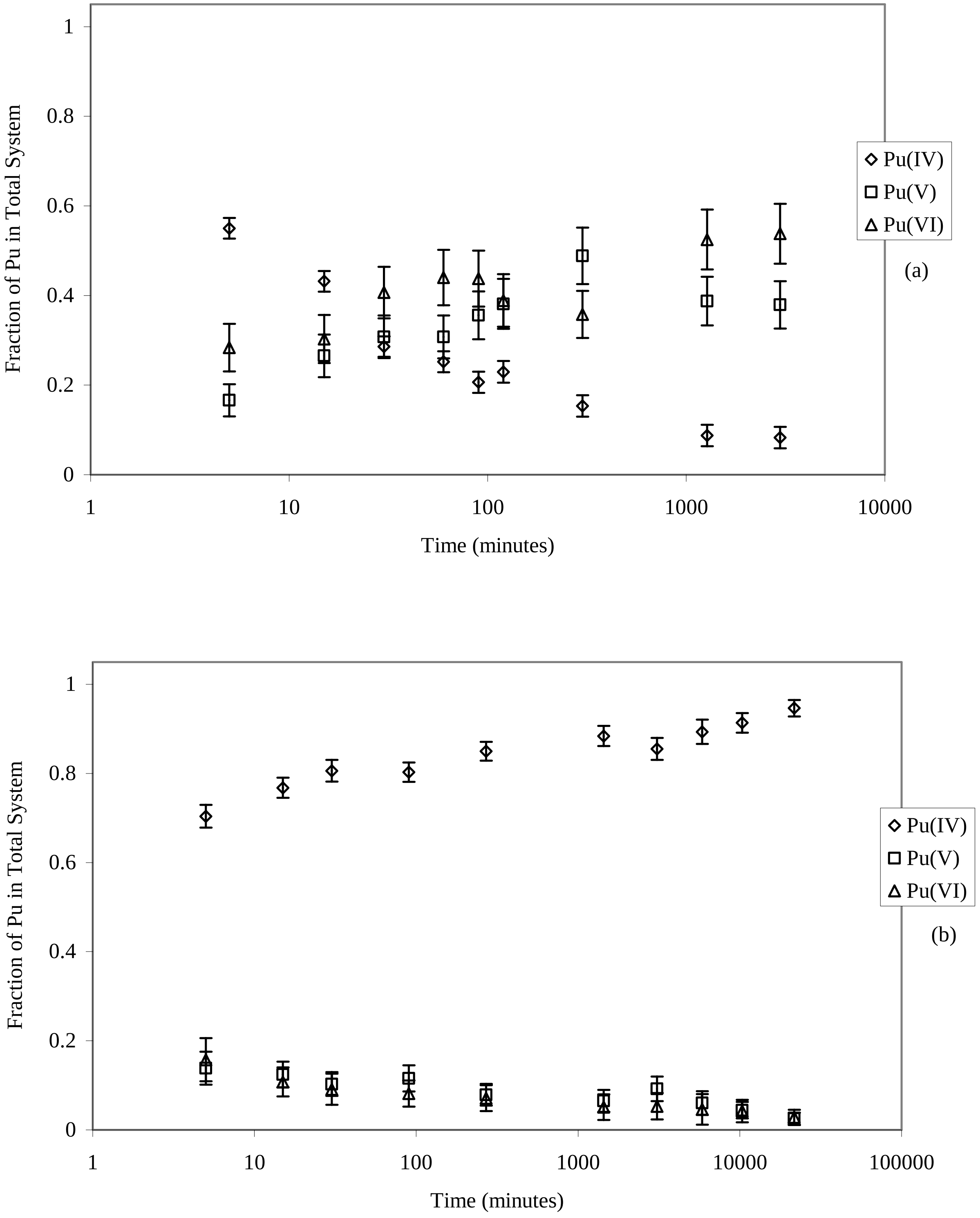

FIGURE 3: Total system Pu oxidation state distribution in pyrolusite suspensions at (a) pH 2.59 ± 0.04 and (b) pH 8.22 ± 0.04 [pyrolusite] = 10.0 ± 0.1 $m^2\,L^{-1}$ (4.00 ± 0.04 g L^{-1}); [NaCl] = 0.01 M; initially added Pu(IV) at [Pu] = 6.1 x 10^{-11} M).

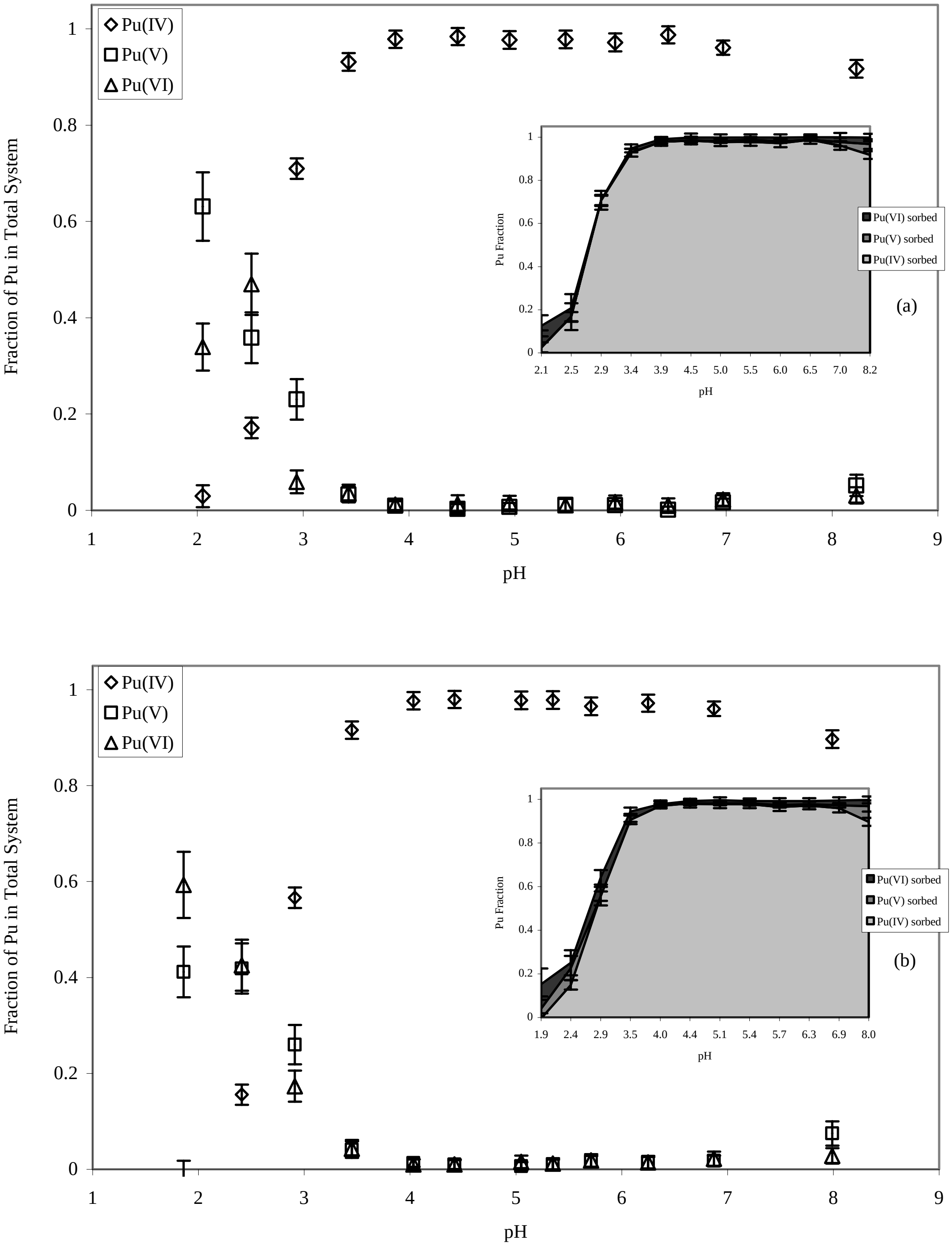

FIGURE 4: Total system oxidation state distribution versus pH after 30 days in (a) initially Pu(IV) and (b) initially Pu(V) pyrolusite systems. Inserts show fraction sorbed an in aqueous phase; unshaded region above curve represents Pu fraction in aqueous phase. ([pyrolusite] = 9.9 ± 0.3 $m^2 L^{-1}$ (3.92 ± 0.05 g L^{-1}); [NaCl] = 0.01 M).